The Reactions of O(^{3}P) with Terminal Alkenes: The H_2CO Channel via 3,2 H-Atom Shift†

Hongmei Su,* Shaolei Zhao, Kunhui Liu, and Tiancheng Xiang

State Key Laboratory of Molecular Reaction Dynamics, and Beijing National Laboratory for Molecular Sciences (BNLMS), Institute of Chemistry, Chinese Academy of Sciences, Beijing 100080, People's Republic of China

Received: May 23, 2007; In Final Form: July 30, 2007

The step-scan time-resolved FTIR emission spectroscopy is used to characterize systematically the H_2CO channel for the reactions of O(^{3}P) with various alkenes. IR emission bands due to the products of CO, CO_2, and H_2CO have been observed in the spectra. H_2CO is identified to be the primary reaction product whereas CO and CO_2 are secondary reaction products of O(^{3}P) with alkenes. A general trend is observed in which the fraction yield of the H_2CO product increases substantially as the reactant alkene varies from C_2H_4, C_3H_6, 1-C_4H_8, iso-C_4H_8, to 1-C_5H_{10}. The formation mechanism of the H_2CO is therefore elucidated to arise from a 3,2 H-atom shift followed by breaking of the C_1-C_2 bond in the initially formed energized diradical RCH_2-$CHCH_2O$*. The 3,2 H-atom shift may become the dominant process with the more rapid delocalization of the energy when the hydrocarbon chain of the alkene molecule is lengthened.

1. Introduction

Reactions of the oxygen atom with alkenes have been attracting long-time attention constantly due to their importance to atmospheric chemistry and combustion chemistry. The identification of reaction channels is of great help to understand the reaction mechanism and therefore to improve realistic conditions, such as combustion efficiency. As is well-known, small unsaturated hydrocarbons such as C_2H_2, C_2H_4, C_3H_4, and C_3H_6 are crucial intermediates in hydrocarbon flames.[1,2] These small unsaturated hydrocarbons mainly, if not dominantly, react with triplet ground-state oxygen atoms. These reactions are believed to play key roles in the generation of polycyclic aromatic hydrocarbons and soot.[3] In this work, our main aim is to study the formaldehyde channel of the reactions of O(^{3}P) with a series of alkenes.

Dating back to the early 1950s, Cvetanovic and co-workers carried out pioneering studies of the reactions of O(^{3}P) with alkenes in the gas phase.[4−10] They found that the reaction proceeds readily with the initial attachment of the electrophilic O atom to the less-substituted carbon atom of the double bond, forming a ketocarbene. In recent years, Bersohn's group performed a series of detailed studies of the reaction products of O(^{3}P) with alkenes.[11−15] A general reaction mechanism was suggested in which O(^{3}P) initially undergoes an electrophilic addition onto the C=C bond, forming a triplet diradical ketocarbene RCH_2CHCH_2O which either decomposes directly to a variety of final products such as vinoxy CH_2CHO or carries out intersystem crossing (ISC) to form a singlet diradical. In the singlet state, the barrier to the 1,2 H-atom shift is lowered dramatically, and the energized intermediate can give rise, through the 1,2 H-atom migration and dissociation, to final products such as HCO. Several channels are identified

$$RCH_2CH{=}CH_2 + O(^3P) \rightarrow HCO + RCH_2CH_2 \quad (1a)$$

$$\rightarrow CH_2CHO + RCH_2 \quad (1b)$$

$$\rightarrow H + RCH_2CHCHO \quad (1c)$$

$$\rightarrow OH + RCHCHCH_2 \quad (1d)$$

where R is a H atom or alkyl radical. When probing the HCO channel using cavity ring-down spectroscopy, they also observed that the branching ratio of channel 1a decreases rapidly with the increasing length of R. For the reactions of O(^{3}P) with ethylene, propene, and other alkenes (including 1-C_4H_8, *cis*-2-C_4H_8, iso-C_4H_8, 1-C_5H_{10}, allene, 1,3-C_4H_6, cyclopentene, and cyclohexene), the HCO channel branching ratios were 0.71 ± 0.16, 0.05 ± 0.02, and 0, respectively.[12] To explain this observation, they proposed that other channels, such as the H_2CO channel, tend to contribute larger fractions to the reaction as the hydrocarbon chain of the alkene molecule lengthens.

Most recently, another three studies were carried out on the reaction of the oxygen atom with the simplest alkene, C_2H_4. By means of IR emission spectroscopy, James et al.[16] observed the vibrationally excited products of HCO, H_2CO, CO, and CO_2 from the 193 nm laser irradiation of the $SO_2-C_2H_4-Ar$ mixture, and they ascribed the formation of CO and CO_2 to the secondary reactions of O(^{3}P) with ethylene. Their study mainly focused on the secondary reactions forming CO and CO_2 but did not deal with the H_2CO product channel. Using the crossed molecular beam scattering technique with soft electron ionization, Casavecchia et al.[17] observed the exoergic channels of the O(^{3}P) + C_2H_4 reaction and measured the relative branchingratios to be 0.27 ± 0.06, 0.01 ± 0.005, 0.13 ± 0.03, 0.47 ± 0.09, and 0.16 ± 0.08 for the channels 2a−2e, respectively.

† Part of the "Sheng Hsien Lin Festschrift".

* To whom correspondence should be addressed. E-mail: hongmei@iccas.ac.cn.

10.1021/jp073993x CCC: $37.00
Published on Web 08/18/2007

$$O(^3P) + C_2H_4 \rightarrow H + CH_2CHO \quad \Delta H = -71 \text{ kJ mol}^{-1} \quad (2a)$$

$$\rightarrow H + CH_3CO \quad \Delta H = -114 \text{ kJ mol}^{-1} \quad (2b)$$

$$\rightarrow H_2 + CH_2CO \quad \Delta H = -356 \text{ kJ mol}^{-1} \quad (2c)$$

$$\rightarrow CH_3 + HCO \quad \Delta H = -113 \text{ kJ mol}^{-1} \quad (2d)$$

$$\rightarrow CH_2 + H_2CO \quad \Delta H = -29 \text{ kJ mol}^{-1} \quad (2e)$$

Interestingly, their measurement shows that a substantial amount of H_2CO is formed. This is opposed to the general notion that the CH_2CHO channel (2a) and the HCO channel (2d) are the only two major reaction channels of the O(^{3}P) + C_2H_4 reaction.[18] The potential energy surface of the O(^{3}P) + C_2H_4 reaction was theoretically investigated by Nguyen et al. using various quantum chemical methods, including G3, CBS-QB3, G2M(CC, MP2), and MRCI.[19] The major products (with predicted yields at $T = 300/2000$ K) were CH_3 + HCO (48/37%), H + CH_2CHO (40/19%), and $CH_2(X^3B_1)$ + H_2CO (5/29%). The calculation also showed that the reaction of the O(^{3}P) with C_2H_4 leads to the product of H_2CO but the yield of the H_2CO channel is relatively low at room temperature.

For larger alkenes, Oguchi et al. investigated the mechanism of reactions of O(^{3}P) with three isomeric butenes (*trans*-2-, iso-, and 1-butene).[20] They measured the yields of the CH_3 and C_2H_5 radical products using photoionization mass spectrometry. For isobutene, the fractions of CH_3 and C_2H_5 channel were 0.24 ± 0.08 and 0.29 ± 0.05, respectively. The total fraction yield of the CH_3 and C_2H_5 products were 0.53. For 1-butene, the total yield of the CH_3 and C_2H_5 products was only 0.10. The rest of the channels accounting for a large fraction remained suspensive.

Zhao et al.[21] calculated the reaction pathways of the O(^{3}P) with isobutene using the unrestricted second-order Møller−Plesset perturbation (UMP2) and complete basis set CBS-4M level of theory methods. They predicted the major product channels to be $CH_2C(O)CH_3$ + CH_3, *cis*-/*trans*-CH_3CHCHO + CH_3, $(CH_3)_2CCO$ + H_2, and $CH_3C(CH_2)_2$ + OH, among which $(CH_3)_2CCO$ + H_2 was the energetically most favorable one. In addition, they predicted that the product channel $(CH_3)_2C$ + H_2CO is only of minor contribution.

To sum up, previous experimental investigations either observed directly the formation of the H_2CO product[16,17] for the O(^{3}P) + C_2H_4 reaction or indicated the existence of such a channel for the reactions of O(^{3}P) with larger alkenes.[12] In addition, theoretical calculations[19,21] predicted the H_2CO channel with a minor fraction yield at room temperature. The question arises whether the H_2CO product channel is common to the serial reactions of O(^{3}P) with alkenes, and what is the mechanism underlying the formation of H_2CO. In the present paper, we have investigated systematically the H_2CO channel for the reactions of O(^{3}P) with various alkenes by means of step-scan time-resolved FTIR emission spectroscopy. A general trend is observed in which the fraction yield of the H_2CO product increases substantially as the reactant alkene varies from C_2H_4, C_3H_6, 1-C_4H_8, iso-C_4H_8, to 1-C_5H_{10}. An alternative scenario for the reaction of O(^{3}P) with alkenes is revealed in which, as the hydrocarbon chain of the alkene molecule is lengthened, the initially formed energized intermediate ketocarbene RCH_2-$CHCH_2O$* involves more rapid delocalization of the energy, and thus, the 3,2 H-atom shift followed by breaking of the C_1−C_2 bond may become the dominant process which leads to the formation of the final product H_2CO.

2. Experimental Section

The reaction products are monitored by step-scan time-resolved Fourier transform emission spectroscopy.[22] A step-scan FTIR spectrometer is commercially available but requires significant modification for coupling with a pulsed laser and applying it to the study of laser-initiated free-radical reactions. This newly upgraded machine comprises a Nicolet Nexus 870 step-scan FTIR spectrometer, a Lambda Physik (LPX305i) Excimer laser, and a pulse generator (Stanford Research DG535) to initiate the laser pulse and achieve synchronization of the laser with the data collection, two digitizers (internal 100 kHz 16 bit digitizer and external 100 MHz 14 bit GAGE 8012A digitizer), which offer fast time resolution and a wide dynamic range as needed, and a personal computer to control the whole experiment. The detector used in this experiment is a liquid-nitrogen-cooled InSb detector.

The reaction is initiated in a stainless steel flow reaction chamber. A pair of parallel multilayer coated mirrors (reflectivity $R > 0.95$ at 351 nm) reflect the UV laser beam multiple times to increase the photolysis zone. O(^{3}P) atoms are produced via the laser photodissociation of NO_2 at 351 nm (XeF laser, Lambda Physik LPX305i, ~50 mJ cm^{-2}). Only the ground-state O(^{3}P) atoms are produced following the 351 nm photolysis of NO_2, and there is no interference from O(^{1}D) atoms. Typically, 250 mTorr of alkenes (≥99.5%) and 150 mTorr of NO_2 (≥99.9%) enter the flow chamber 1 cm above the photolysis beam via needle valves. The chamber is pumped by an 8 L s^{-1} mechanical pump, and the stagnation pressure of the chamber is measured by a MKS capacitance monometer. The constant pressure of sample is maintained by adjusting the pumping speed and the needle valves. Transient infrared emission is collected by a pair of gold-coated White-Cell spherical mirrors and collimated by a CaF_2 lens to the step-scan Fourier spectrometer. The spectrometer and the collimating tube are both flushed with N_2 to eliminate the environmental CO_2 absorption. Alkenes were purchased from Aldrich and used as received.

3. Results and Discussion

3.1. Identification of the Reaction Products from IR Emission Spectra. In the first reference experiment, when pure alkenes were irradiated by a 351 nm laser, no IR emission was observed. This is expected because alkenes cannot be photolyzed by a 351 nm laser.

In the second reference experiment, when pure NO_2 was irradiated by a 351 nm laser, the IR emission due to the photofragment NO spanning from 1790 to 1970 cm^{-1} was observed, as shown in Figure 1 with the three-dimensional "waterfall" view of the emission spectra at selected time delays following laser excitation of the pure NO_2. Photodissociation of NO_2 at 351 nm produces vibrationally excited NO and the O(^{3}P) atom

$$NO_2 + h\nu\,(351 \text{ nm}) \rightarrow NO + O(^3P) \quad (3)$$

Fortunately, the NO spectral region is isolated and will not interfere with the detection of the products of O(^{3}P) with alkenes, which usually cover the spectral region higher than 1970 cm^{-1}.

When the flowing gaseous mixture of the O(^{3}P) precursor, NO_2, with alkenes was irradiated by a 351 nm laser, intense IR emissions were observed. As an example, Figure 2 shows the three-dimensional waterfall views of the IR emission spectra at selected time delays following laser excitation of the NO_2/iso-C_4H_8 mixture. Similarly, the time-resolved IR emission

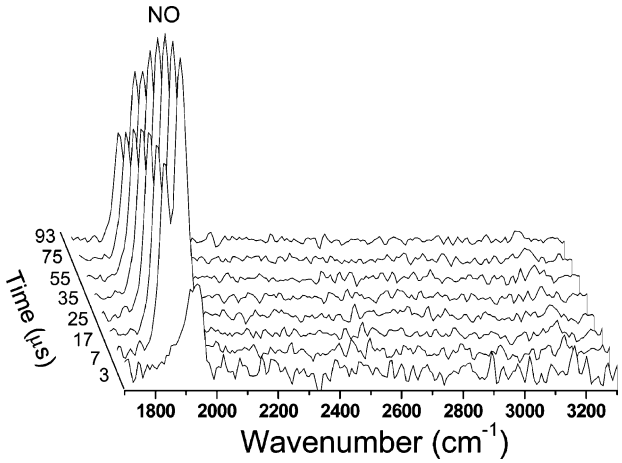

Figure 1. Time-resolved IR emission spectra at selected time delays of 3, 7, 17, 25, 35, 55, 75, and 93 μs following the 351 nm photodissociation of NO_2 in the 1700−3300 cm^{-1} region with 16 cm^{-1} resolution.

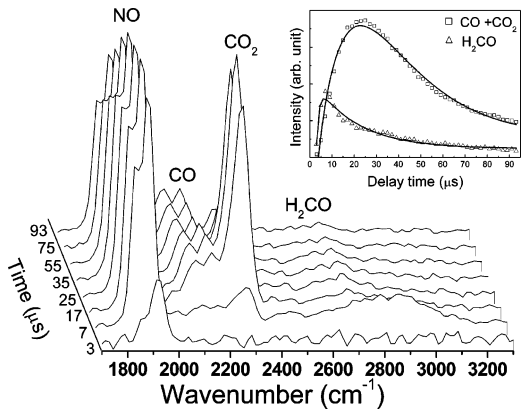

Figure 2. Time-resolved IR emission spectra at selected time delays of 3, 7, 17, 25, 35, 55, 75, and 93 μs following the 351 nm irradiation of the NO_2−iso-C_4H_8 mixture in the 1700−3300 cm^{-1} region with 32 cm^{-1} resolution. The inset shows the time evolution of the peak area of the two IR emission bands of H_2CO and CO/CO_2. The triangle spots are the experimental peak area of the H_2CO emission band, and the square spots are the experimental data of the CO/CO_2 emission band. The solid curves are the fitting results.

spectra were collected for the reactions of $O(^3P)$ with various alkenes including C_2H_4, C_3H_6, 1-C_4H_8, iso-C_4H_8, 1-C_5H_{10}, and 1,3-C_4H_6. To compare explicitly the products of these reactions, the specific time slices of the IR emission spectra for various alkenes are displayed in Figure 3. The IR emissions arise from the vibrationally excited products from the reactions of $O(^3P)$ with alkenes. These reaction products can be identified from spectral assignment.

TR-FTIR emission spectra record the infrared fluorescence emitted from vibrationally excited species due to a set of vibrational transitions $\nu \rightarrow \nu - 1$, which consists of numerous rotational transitions. Therefore, the IR emission band is generally much broader than normal static IR absorption spectra, and the peak center exhibits a somewhat red shift relative to the fundamental frequency position ($1 \rightarrow 0$). Collected with a spectral resolution of 16 cm^{-1}, only the contour due to the numerous overlapping rovibrational transitions can be obtained. The rotational structure cannot be resolved.

Judging from its spectral position, the emission band spanning from 2050 to 2380 cm^{-1} is attributed to the overlapping CO emission (fundamental band at 2143 cm^{-1}) and CO_2 emission (fundamental band at 2349 cm^{-1}). As will be discussed, CO and CO_2 are formed mainly from the secondary reactions of

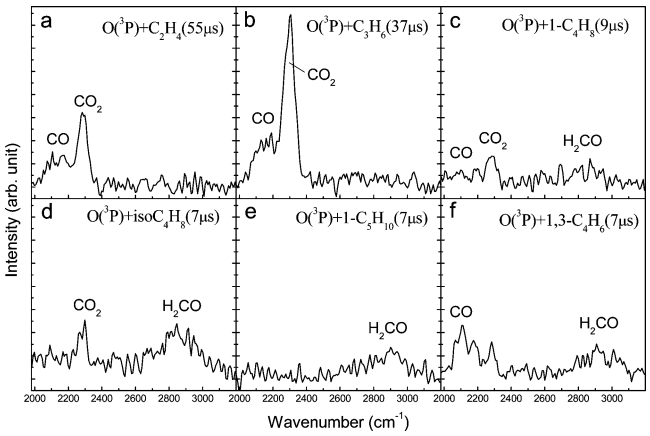

Figure 3. IR emission spectra for the reactions of $O(^3P)$ with six different alkenes at typical reaction times: (a) C_2H_4, (b) C_3H_6, (c) 1-C_4H_8, (d) iso-C_4H_8, (e) 1-C_5H_{10}, and (f) 1,3-C_4H_6. Figure 3a and b shows the spectra at the reaction time when the CO/CO_2 bands reach their maximum intensity. Figure 3c−f shows the spectra at the reaction time when the H_2CO band reaches its maximum intensity.

$O(^3P)$ + alkenes. Another broad emission band from 2600 to 3100 cm^{-1} is assigned to both vibrationally excited H_2CO $\Delta\nu_5 = -1$ (b-type CH_2 asymmetric stretch mode: 2843 cm^{-1})[23] and $\Delta\nu_1 = -1$ (a-type CH_2 symmetric stretch mode: 2783 cm^{-1})[23] bands. Although falling into the same spectral region, this band is not likely arising from other possible products such as CH_3 (a′-type CH stretch mode: 3004 cm^{-1})[23] or C_2H_5 (a′-type CH stretch mode: 2854 cm^{-1}; a′-type CH_2 symmetric stretch mode: 3037 cm^{-1}; a′-type CH_3 symmetric stretch mode: 2875 cm^{-1}).[23] It is known that the dominant reaction channels of $O(^3P) + C_2H_4$ and $O(^3P) + C_3H_6$ are to form CH_3 and C_2H_5.[12,18] However, as shown in Figure 3a and b, no emission signals can be observed in the spectral region (2600−3100 cm^{-1}) where CH_3 or C_2H_5 should be present. On the other hand, it has been observed that the fraction yield of the CH_3 and C_2H_5 channel decreases with the increasing size of the alkene molecule.[12] Therefore, if no CH_3 or C_2H_5 is observed for the $O(^3P) + C_2H_4$ and $O(^3P) + C_3H_6$ reactions in the IR emission spectra, there are no chances for observing the CH_3 or C_2H_5 emission for the reaction of $O(^3P)$ with larger alkenes. The emission bands from 2600 to 3100 cm^{-1} observed in Figure 3c−e are arising from other reaction products, most likely, H_2CO. James et al. also observed and assigned this emission band to the ν_1 and ν_5 vibrationally excited H_2CO when studying the reaction of $O(^3P)$ with C_2H_4.[16] The reason why no IR emissions from the CH_3 or C_2H_5 were observed should be due to their small Einstein A coefficient [CH_3 (7.5 s^{-1})][24] or their low vibrational excitation. In contrast, the Einstein A coefficient of H_2CO is large (73.2 s^{-1} for ν_1 and 88.6 s^{-1} for ν_5).[25] IR emission spectroscopy is thus a sensitive probe for H_2CO but not for CH_3 and C_2H_5.

3.2. Identification of H_2CO as the Primary Product and CO/CO_2 as the Secondary Products of the $O(^3P)$ + Alkene Reactions. The inset in Figure 2 plots the IR emission intensity of the peak area as a function of the reaction time. The rise reflects the product formation, and the decay is due to vibrational relaxation and removal from the observation zone. The diffusion effect causing the removal from the observation zone can be neglected on the time scale of hundreds of microseconds.[26] Therefore, the rise and fall of the IR emission temporal curves are fitted with a sum of two exponentials $y_0 + C(\exp(-k_1 t) - \exp(-k_2 t))$, providing information on the kinetics of the product formation and vibrational relaxation. The typical fitting results are shown in the inset of Figure 2. Satisfactory fitting results are obtained although the model is greatly simplified without

considering complications such as product molecules populated at ground vibrational level ($v = 0$) not being detected by IR emission spectroscopy.[27]

It is estimated that only a small amount (approximately 5%) of NO_2 molecules are dissociated upon 351 nm laser irradiation at a power of 50 mJ cm^{-2}, leading to [O(^{3}P)] $\approx 2 \times 10^{14}$ molecules/cm^3. The concentration range of [iso-C_4H_8] $= 3 \times 10^{15}-1 \times 10^{16}$ molecules/cm^3 is sufficiently in excess to ensure pseudo-first-order conditions. The rate of the rise of product formation from the reaction of O(^{3}P) with iso-C_4H_8 is therefore given by $k' = k$[iso-C_4H_8]. The biexponential fitting yields a formation rate constant of 8.5×10^{-12} cm^3 molecule^{-1} s^{-1} for H_2CO and 3.4×10^{-12} cm^3 molecule^{-1} s^{-1} for CO/CO_2. The formation rate constant of H_2CO agrees well with the reported overall rate constant of 1.8×10^{-11} cm^3 molecule^{-1} s^{-1} for the reaction of O(^{3}P) with iso-C_4H_8.[28] Consequently, H_2CO can be concluded to be the primary reaction product from the O(^{3}P) + iso-C_4H_8 reaction. In contrast, the formation of CO/CO_2 lags behind that of H_2CO, corresponding to a rate constant of 3.4×10^{-12} cm^3 molecule^{-1} s^{-1}, which is much smaller than the overall reaction rate constant of O(^{3}P) with iso-C_4H_8. This indicates that CO and CO_2 are most likely produced from secondary reactions of O(^{3}P) + alkenes, that is, the consecutive reaction of the primary products causing the formation delay of CO/CO_2. Previous investigations also show that a negligible amount of CO is produced directly from the reactions of O(^{3}P) + alkenes.[11,17,20] Similar kinetics analysis is applied to the other O(^{3}P) + alkene reactions, and it all shows that H_2CO is the primary product and CO/CO_2 are secondary products.

3.3. Possible Secondary Reactions. Although it is a versatile and powerful means of observing the IR-active products in a reaction mixture, the IR emission detection has the disadvantage of low sensitivity relative to other detection methods. Thus, the species' partial pressures are necessarily relatively high to ensure adequate signal-to-noise ratios for detection purposes. Under these conditions, secondary chemistry usually plays a role in the production of IR-active species.

The primary reactions of O(^{3}P) + alkenes lead to some radical products, including CH_3, C_2H_5, CH_2CHO, HCO, and H atoms. Due to the low concentration of these radicals, secondary radical−radical reactions are negligible, while secondary reactions of the abundant alkene or NO_2 molecules with these primary radicals such as $CH_3 + NO_2$, $CH_2CHO + NO_2$, HCO + alkenes, and $HCO + NO_2$ are likely to contribute to the formation of the observed IR-active products and have to be considered.

The first IR-active product H_2CO has been identified to be generated from the primary reactions of O(^{3}P) + alkenes by kinetics analysis. Still, the following possible secondary reactions are considered and eliminated as a source for generating H_2CO. The reaction of HCO + alkenes can be ruled out due to its extremely small reactivity (k on the order of 10^{-17} cm^3 molecule^{-1} s^{-1} [29]). The $CH_2CHO + NO_2$ reaction does not produce H_2CO but proceeds through other pathways, as suggested by Barnhard et al.'s study[30]

$$CH_2CHO + NO_2 \rightarrow O_2NCH_2CHO \quad (4a)$$

$$\rightarrow CH_2CO + HONO \quad (4b)$$

The $CH_3 + NO_2$ reaction only produces a negligible amount of H_2CO. Yamada,[31] Wollenhaupt,[32] and Biggs[33] have identified the reaction channels 5a, 5b, and 5c, but none of these studies have observed the product H_2CO from the reaction of $CH_3 + NO_2$. The theoretical calculation by Biggs[33] predicted that the H_2CO channel yielded from $CH_3 + NO_2$ is a factor of 50 smaller than the major CH_3O channel (5a)

$$CH_3 + NO_2 \rightarrow CH_3O + NO \quad (5a)$$

$$\xrightarrow{M} CH_3NO_2 \quad (5b)$$

$$\xrightarrow{M} CH_3ONO \quad (5c)$$

$$\rightarrow H_2CO + HNO \quad (5d)$$

For the other observed IR-active products CO and CO_2, the kinetics analysis already shows that they are due to the secondary reactions of O(^{3}P) + alkenes. After analyzing the expected products of possible secondary reactions, it is found that the reaction of $HCO + NO_2$ is the most probable secondary reaction for generating the products of CO and CO_2.

HCO radicals are known to react with NO_2 rapidly with a rate constant of $2.7-5.7 \times 10^{-11}$ cm^3 molecule^{-1} s^{-1}.[34] Recently, Meyer et al.[35] experimentally studied the products of the reaction of HCO with NO_2, suggesting seven reaction channels

$$HCO + NO_2 \rightarrow HONO + CO \quad (6a)$$

$$\rightarrow OH + NO + CO \quad (6b)$$

$$\rightarrow HNO + CO_2 \quad (6c)$$

$$\rightarrow H + NO + CO_2 \quad (6d)$$

$$\rightarrow HCO_2 + NO \quad (6e)$$

$$\xrightarrow{M} HC(O)NO_2 \quad (6f)$$

$$\xrightarrow{M} HC(O)ONO \quad (6g)$$

Due to the dissociation of HCO_2 to form H and CO_2 with only a low activation barrier, the reaction channel 6e is, in effect, indistinguishable from 6d. The branching ratios yielding CO and CO_2 were found to be $(k_{6a} + k_{6b})/k_6 = (0.66 \pm 0.10)$ and $(k_{6c} + k_{6d} + k_{6e})/k_6 = (0.34 \pm 0.10)$, respectively. Rim et al. also measured the branching ratios forming CO + NO + OH and H + NO + CO_2 to be 63 ± 5 and $37 \pm 5\%$, respectively.[34] Guo et al.[36] determined the yield fractions of CO_2 to be $52 \pm 10\%$ and estimated that of CO to be $48 \pm 10\%$ from the HCO + NO_2 reaction. All of these studies have identified that the reaction of $HCO + NO_2$ produces dominantly CO and CO_2. Since HCO is also a major primary product from O(^{3}P) + alkenes reactions, the secondary reaction of $HCO + NO_2$ is the most probable source for generating CO and CO_2 observed in the IR emission spectra.

Although we are targeting our study to the reaction of O(^{3}P) + alkenes in this work, the secondary reactions cannot be avoided because of the presence of the reactive primary radical products, that is, HCO in this case, to react with NO_2, forming observable products of CO and CO_2. On the other hand, the products CO and CO_2 are presumably mainly correlated with the primary HCO channel from the O(^{3}P) + alkene reactions. We can therefore elucidate the relative yield of the HCO channel by measuring the yield of CO and CO_2.

3.4. The Relative Yield of the H_2CO Channel to the HCO Channel. In the O(^{3}P) + alkenes reactions, as the hydrocarbon chain lengthens from C_2H_4, C_3H_6, 1-C_4H_8, iso-C_4H_8, to 1-C_5H_{10}, one obvious trend can be observed from Figure 3 in which the fraction yield of the H_2CO channel relative to the HCO channel (reflected by the CO/CO_2 emission intensity in the spectra)

TABLE 1: Peak Areas of the IR Emission Bands of H_2CO (A_1) and CO/CO_2 (A_2) at Their Maximum for Various $O(^3P)$ + Alkene Reactions

reactions	$A_1(H_2CO)$	$A_2(CO + CO_2)$	A_1/A_2
$O(^3P) + C_2H_4$	0	45.1	0
$O(^3P) + C_3H_6$	0	93.6	0
$O(^3P) + 1\text{-}C_4H_8$	25.5	23.5	1.1
$O(^3P) + iso\text{-}C_4H_8$	70.9	52.6	1.3
$O(^3P) + 1\text{-}C_5H_{10}$	40.3	10.7	3.7
$O(^3P) + 1,3\text{-}C_4H_6$	38.9	39.6	1.0

increases. The peak area of the H_2CO emission band (A_1) divided by that of the CO/CO_2 band (A_2) can be used to exhibit the trend of the fraction yield of the H_2CO channel relative to that of the HCO channel varying with alkenes. These ratios are listed in Table 1. For the $O(^3P) + C_2H_4$ and $O(^3P) + C_3H_6$ reactions, no H_2CO products were observed, indicating a negligible yield of H_2CO from these two reactions. In contrast, a noticeable amount of H_2CO was observed for the $O(^3P) + 1\text{-}C_4H_8$, and the yield increased substantially for the $O(^3P) + iso\text{-}C_4H_8$ reaction and the $O(^3P) + 1\text{-}C_5H_{10}$ reaction. Interestingly, H_2CO was also observed from the reaction of $O(^3P)$ with the diene $1,3\text{-}C_4H_6$.

3.5. The Reaction Mechanism forming H_2CO from the $O(^3P)$ + Alkene Reactions. The reaction product channels for various $O(^3P)$ + alkene reactions have been well studied by Bersohn's group.[11−15] They have proposed the following reaction mechanism, which has been validated by several quantum chemical calculations.[19,21]

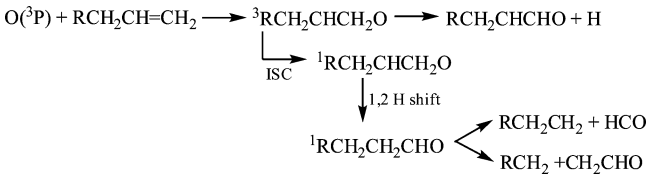

The reaction starts with the addition of the electrophilic oxygen atom to the C=C double bond, forming a triplet diradical ketocarbene. The triplet diradicals either decompose to products (by H− loss) or undergo intersystem crossing (ISC) to singlet diradicals. The 1,2 H-atom shift for the triplet diradicals is found to confront a large barrier height which cannot be surmounted energetically. The direct decomposition on the triplet surface dominates. The singlet diradicals produced from the triplet ketocarbene upon ISC may rearrange by a 1,2 H-atom shift, forming a "hot" aldehyde intermediate. The energized aldehyde dissociates rapidly into various products, including the two main channels of $RCH_2CH_2 + HCO$ and $RCH_2 + CH_2CHO$. For the simplest alkene C_2H_4 reacting with $O(^3P)$, it is now clear that approximately half of the reaction channels occur on the triplet surface and half on the singlet surface.[17,19]

To interpret the formation of the H_2CO channel observed in the present work, we turn to the quantum chemical calculation results that have been reported. For the $O(^3P) + C_2H_4$ reaction, Peeters's calculation can explain quite well the formation mechanism of H_2CO.[19] Their calculation shows that there is a sizable yield of H_2CO, and this channel occurs on the triplet surface via the direct dissociation of the initially formed diradical CH_2CH_2O. However, for larger alkenes reacting with $O(^3P)$, it is lack of such explicit quantum chemical calculation results interpreting the formation of H_2CO. Only Zhao's calculation on the reaction of $O(^3P) + iso\text{-}C_4H_8$ provides some hints about the H_2CO formation mechanism.[21] First, they found that on the triplet surface, the H_2CO formation involves overcoming a barrier of 96.6 kJ mol^{-1} higher than the energy of the reactants and thus is energetically forbidden. Second, on the singlet surface following the ISC of the triplet ketocarbene $(CH_3)_2CCH_2O$ to its singlet state and a 1,2 H-atom shift, the intermediate aldehyde $(CH_3)_2CHCHO$ is formed and undergoes further rearrangement via the H-atom shift back from the C2 atom to the C1 atom and a ring closure to form an epoxide $(CH_3)_2C-O-CH_2$ (ring structure). Following the ring opening and bond fission, the final product H_2CO is formed. This reaction route via the epoxide on the singlet surface involves proceeding through multiple steps of molecular rearrangements and overcoming high-energy barriers and thus seems not to be a feasible mechanism to account for the formation of H_2CO.

Min et al.[12] proposed the possible existence of the H_2CO channel for larger alkenes reacting with $O(^3P)$. When studying the HCO channels for different alkenes by cavity ring-down spectroscopy, they observed substantial HCO formed from the $O(^3P) + C_2H_4$ reaction, a much smaller amount from the $O(^3P) + C_3H_6$ reaction, but nothing from other larger alkenes. To account for this phenomenon, they proposed that for larger alkene reactions, a hydrogen atom migrates rather from C3 to C2, followed by breaking of the C_1-C_2 bond

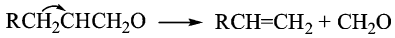

but not from C1 to C2 followed by breaking of the C_1-C_2 bond Their experiments provide nice clues, motivating us to search

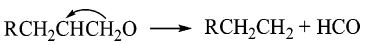

for the existence of this H_2CO channel. Indeed, we have observed directly the H_2CO products from various $O(^3P)$ + alkene reactions and found that the relative yield of the H_2CO channel to that of the HCO channel increases with the increasing hydrocarbon chain length of the alkene molecules. This trend is in good agreement with the HCO yield varying with alkene molecules observed by Bersohn's group.[12] Combining the findings of our study with theirs, one conclusion can be naturally drawn that the 3,2 H-atom shift channel forming H_2CO products is becoming dominant over the 1,2 H-atom shift channel forming HCO products with the increasing size of the alkene molecules. It is therefore fascinating to analyze the underlying mechanism which governs the preference of the hydrogen-atom migration process.

First, it is noticeable that the reaction channel forming H_2CO is highly exothermic compared to the HCO channel. This is because two stable molecules, rather than two unstable radicals, are produced. The much higher exothermicity might result in some thermodynamic bias of the H_2CO channel.

For the series of $O(^3P)$ + alkene reactions, as the hydrocarbon chain of the alkene molecule is lengthened, more rapid delocalization of the energy is expected to occur in the initially formed diradical $RCH_2CHCH_2O^*$. The unimolecular decomposition is thus allowed full scope, and the 3,2 H-atom shift may become the dominant process because so much more energy is released in that channel. As shown in Table 2, the exothermicity of the H_2CO channel increases dramatically from C_2H_4 to C_3H_6, but there is only a slight increase from C_3H_6 to $1\text{-}C_5H_{10}$. On the other hand, we have observed that the relative yield of the H_2CO channel increases substantially from C_3H_6 to $1\text{-}C_4H_8$, $iso\text{-}C_4H_8$, and $1\text{-}C_5H_{10}$, suggesting that there are other factors playing significant roles in the 3,2 H-atom shift process besides the factor of the reaction exothermicity.

Considering the 1,2 H-atom shift process for different alkenes, the R group bonded to the C-2 atom is expected to generate some steric hindrance. As listed in Table 2, the steric hindrance

TABLE 2: Possible Underlying Factors Leading to the Preference of the Hydrogen Atom Migration Process Involved in the Reactions of O(^{3}P) with Alkenes

alkene	exothermicity[a]	R group causing steric hindrance for the 1,2 H-atom shift[b]	C_3-H bond energy of the alkene[c,37]
$CH_2=CH_2$	−19.8	H	
$CH_3-CH=CH_2$	−325.4	CH_3	369
$CH_3CH_2-CH=CH_2$	−337.9	CH_3CH_2	350.6
$(CH_3)_2-C=CH_2$	−320.9	$(CH_3)_2$	362.8
$CH_3(CH_2)_2-CH=CH_2$	−336.6	$CH_3CH_2CH_2$	345.2

[a] Exothermicity (in kJ mol^{-1}) of the H_2CO channel of the O + alkene reaction; the enthalpies of formation originated from ref 38. [b] Steric hindrance effect caused by the group attached to the C2 atom of the hot diradical, $RCHCH_2O$. [c] C_3-H bond energy of the alkene, in kJ mol^{-1}.

for the 1,2 H-atom shift is expected to increase with the increasing size of the R group. As a result, the 1,2 H-atom shift process which leads to the HCO channel becomes less and less important for longer-chain alkenes. Alternatively, the 3,2 H-atom shift process takes over, and the H_2CO channel plays a more significant role. In fact, the observed trend of the increasing yield of H_2CO with longer-chain alkenes agrees quite well with the variation of the steric hindrance.

The allylic C_3-H bond energy decreases when the alkene goes from C_3H_6 and 1-C_4H_8 to 1-C_5H_{10}, as shown in Table 2. Since the 3,2 H-atom shift process somehow involves the cleavage of the C_3-H bond first, it is expected that the weaker the C_3-H bond is, the more easily the 3,2 H-atom shift occurs and, thus, the more product of H_2CO yielded. Thus, the H_2CO yield is increased from C_3H_6 and 1-C_4H_8 to 1-C_5H_{10}. On the other hand, the allylic C_3-H bond energy is not the only factor causing the variation of the H_2CO yield with alkenes. For instance, the C_3-H bond energy of iso-C_4H_8 is between those of C_3H_6 and 1-C_4H_8, but its H_2CO yield exceeds any of them. This indicates that the factor of steric hindrance plays a more significant role. For the iso-C_4H_8 reaction compared to those of C_3H_6 and 1-C_4H_8, the $(CH_3)_2$ group presumably generates much larger steric hindrance for the competing 1,2 H-atom shift channel and thus leads to the increasing yield of the H_2CO channel.

In summary, an overall scenario can be revealed for the formation of the H_2CO products. There exists a H_2CO channel for the O(^{3}P) + alkene reactions, and the fraction yield of this channel increases as the hydrocarbon chain of the alkene lengthens (from C_2H_4, C_3H_6, 1-C_4H_8, iso-C_4H_8, to 1-C_5H_{10}). This channel might occur via a 3,2 H-atom shift in the energized adduct

$$RCH_2\overset{\frown}{C}HCH_2O^*$$

followed by breaking of the C_1-C_2 bond. Opposed to the normally proposed 1,2 H-atom shift

$$RCH_2\overset{\frown}{CH}CH_2O^*$$

followed by the formation of the radical HCO channel, the 3,2 H-atom shift mechanism shows obvious preference as the chain of the alkene lengthens. The reaction exothermicity, structural steric hindrance, and allylic C_3-H bond energy are possible factors causing the bias of the 3,2 H-atom shift over the 1,2 H-atom shift involved in the O(^{3}P) + alkene reactions.

The mechanism we proposed here for the formation of H_2CO via a 3,2 H-atom shift is more straightforward and can explain well the experimentally observed trend of the H_2CO yield varying with alkenes. It is therefore desirable to perform some ab initio calculations to explore the feasibility of this mechanism. Also, interesting questions would emerge such as on which surface would the H_2CO channel occur, the triplet or singlet, and whether the 3,2 H-atom shift process would need to surmount a high-energy barrier on the triplet surface, but the barrier is significantly lowered on the singlet surface just like the already-known behavior of the 1,2 H-shift process. We hope this experimental paper can arouse further related computational studies.

Acknowledgment. This work is financially supported by the National Natural Science Foundation of China (Grant No. 20473100 and No. 20673126), the National Basic Research Program of China, and the Chinese Academy of Sciences.

References and Notes

(1) Glassman, I. *Combustion*, 2nd ed.; Academic Press: FL, 1987.
(2) Gardiner, W. C., Jr. *Combustion Chemistry*; Springer-Verlag: New York, 1984.
(3) Nguyen, T. L.; Peeters, J.; Vereechen, L. *J. Phys. Chem. A* **2006**, *110*, 12166.
(4) Cvetanovic, R. J. *J. Chem. Phys.* **1955**, *23*, 1375.
(5) Cvetanovic, R. J. *Can. J. Chem.* **1955**, *33*, 1684.
(6) Cvetanovic, R. J. *J. Chem. Phys.* **1956**, *25*, 376.
(7) Cvetanovic, R. J. *J. Chem. Phys.* **1959**, *30*, 19.
(8) Cvetanovic, R. J. *J. Chem. Phys.* **1960**, *33*, 1063.
(9) Cvetanovic, R. J. *J. Phys. Chem.* **1970**, *74*, 2730.
(10) Cvetanovic, R. J. *Adv. Photochem.* **1963**, *1*, 115.
(11) Quandt, R.; Min, Z.; Wang, X.; Bersohn, R. *J. Phys. Chem. A* **1998**, *102*, 60.
(12) Min, Z.; Wong, T. H.; Quandt, R.; Bersohn, R. *J. Phys. Chem. A* **1999**, *103*, 10451, and references therein.
(13) Min, Z.; Wong, T. H.; Su, H.; Bersohn, R. *J. Phys. Chem. A* **2000**, *104*, 9941.
(14) Su, H.; Bersohn, R. *J. Chem. Phys.* **2001**, *115*, 217.
(15) Su, H.; Bersohn, R. *J. Phys. Chem. A* **2001**, *105*, 9178.
(16) James, A. D.; Eunsook, S. H.; Karen, J. C.; Gary, D. D. *J. Phys. Chem. A* **2004**, *108*, 10965.
(17) Casavecchia, P.; Capozza, G.; Segoloni, E.; Leonori, F.; Balucani, N.; Gualberto, G. *J. Phys. Chem. A* **2005**, *109*, 3527.
(18) Schmoltner, A. M.; Chu, P. M.; Brudzynski, R. J.; Lee, Y. T. *J. Chem. Phys.* **1989**, *91*, 6926.
(19) Nguyen, T. L.; Vereecken, L.; Hou, X. J.; Nguyen, M. T.; Peeters, J. *J. Phys. Chem. A* **2005**, *109*, 7489, and reference therein.
(20) Oguchi, T.; Ishizaki, A.; Kakuta, Y.; Matsui, H. *J. Phys. Chem. A* **2004**, *108*, 1409.
(21) Zhao, H. M.; Bian, W. S.; Liu, K. *J. Phys. Chem. A* **2006**, *110*, 7858.
(22) Zhu, Q.; Huang, S.; Wang, X. *Chin. J. Chem. Phys.* **1993**, *6*, 87.
(23) NIST Standard Reference Database 69, NIST Chemistry WebBook. http://webbook.nist.gov/chemistry/ (June 2005 release).
(24) Donaldson, D. J.; Stephen, R. L. *J. Chem. Phys.* **1986**, *85*, 817.
(25) Zou, P.; Klippenstein, S. J.; Osborn, D. L. *J. Phys. Chem. A* **2005**, *109*, 4921.
(26) Xiang, T.; Liu, K.; Shi, C.; Su, H.; Kong, F. *Chem. Phys. Lett.* **2007**, *437*, 8.
(27) Osborn, D. L. *J. Phys. Chem. A* **2003**, *107*, 3728.
(28) Adusei, G. Y.; Fontijn, A. *J. Phys. Chem.* **1994**, *98*, 3732.
(29) Lesclaux, R.; Roussel, P.; Veyret, B.; Pouchan, C. *J. Am. Chem. Soc.* **1986**, *108*, 3872.
(30) Barnhard, K. I.; Santiago, A.; He, M.; Asmar, F.; Weiner, B. R. *Chem. Phys. Lett.* **1991**, *178*, 150.
(31) Yamada, F.; Slage, I. R.; Gutman, D. *Chem. Phys. Lett.* **1981**, *83*, 409.
(32) Wollenhaupt, M.; Crowley, J. N. *J. Phys. Chem. A* **2000**, *104*, 6429.
(33) Biggs, P.; Canosa-Mas, C. E; Fracheboud, J.-M; Parr, A. D.; Shallcross, D. E.; Wayne, R. P. *J. Chem. Soc., Faraday Trans.* **1993**, *89*, 4163.
(34) Rim, K. T.; Hershberger, J. F. *J. Phys. Chem. A* **1998**, *102*, 5898, and references therein.
(35) Meyer, St.; Temps, F. *Int. J. Chem. Kinet.* **2000**, *32*, 136.
(36) Guo, Y.; Smith, S. C.; Moore, C. B. *J. Phys. Chem.* **1995**, *99*, 7473.
(37) Lide, D. R. *CRC Handbook of Chemistry and Physics*, 85th ed.; CRC Press: Boca Raton, FL, 2004.
(38) Luo, Y. R. *Handbook of Bond Energies* (in Chinese); Science Press: Beijing, China, 2005.